Analysis of observational data, to calculate the Delayed-Tau model parameters

Dimitrios Papachristopoulos

Table of contents

Abstract

The Star Formation History (SFH) of a galaxy can offer many insights not only for the evolution and the future of the galaxy, but also for the evolution of the Universe. This is why there are various theoretical models trying to describe the SFH of galaxies. One of those models is the Delayed-Tau model, which approximates the Star Formation Rates (SFR) of galaxies as a function with a rising SFR at the beginning, until it reaches a peak at a time τ, unique for each galaxy, and then it drops at an exponential rate.

Haslbauer, Kroupa, and Jerabkova (2023) argue that the Delayed-τ model is opposed to the Lilly-Madau plot ((Madau and Dickinson 2014)), which plots the observed SFR's of galaxies with the corresponding redshifts (z) and calculates a cosmic SFR peak at $z \approx 2$. The way they calculated this inconsistency is by using observatory data for SFR and Stellar Masses from the UNGC catalog (Karachentsev, Makarov, and Kaisina (2013), Karachentsev and Kaisina (2013)) for calculating the parameters (the timescale τ and the normalization constant A_{del}) of the model. This calculation for the galaxies of the Local Cosmological Volume (LCV), allows the investigation of the SFR throughout the life each galaxy and so we can find the expected time of peak of the SFR.

In this thesis project, we will try to calculate the same parameters, by using a bigger sample size and the method Markov Chain Monte Carlo, to examine if the inconsistencies of the model derive from the results of the previous analysis, or if it is an intrinsic problem of the model

Keywords: Galaxies, Galaxy Evolution, Star Formation History (SFH), Star Formation Rate (SFR), Delayed-τ, Local Cosmological Volume, Lilly-Madau Plot, Redshift, Markov Chain Monte Carlo (MCMC).

Galaxy Morphology and Star-Forming Regions

This thesis will focus on how a specific parametric model tries to explain the Star-Formation Histories of galaxies, but to do that, we first need to understand what a galaxy is, what it is made of, the mechanisms of its evolution, and how we can distinguish them.

The study of galaxies is a very active field of astronomy since it is a relatively young discipline. Until 1920, astronomers who observed spiral nebulae were not certain what they were. In 1921, two papers were published: one argued that the Milky Way constituted the whole Universe and that the spiral nebulae were part of it, while the second argued that each spiral nebula was, in fact, a distinct "island universe" (Shapley and Curtis 1921). This debate became known as the Great Debate[1].

In 1925, Edwin Hubble put an end to the debate by showing that the distances to the spiral nebulae were far too great compared to other objects within the Milky Way. The method he used involved observing Cepheid variable stars in these nebulae. By applying the period-luminosity relationship, which had been discovered by Henrietta Swan Leavitt (Leavitt 1907), Hubble was able to determine their distances. This groundbreaking discovery confirmed that spiral nebulae were indeed separate galaxies, marking the beginning of extragalactic astronomy and revolutionizing our understanding of the Universe.

Today we know that galaxies are large-scale structures containing, Stars, gas and dust, Stellar and planetary systems and Stellar remnants (white dwarves, neutron stars and black holes). Those structures are held together by their gravity, having Stellar Masses more than $\sim 10^5 \, M_\odot$, and an average diameter of ~ 4 kpc. They are extremely diverse systems, and each galaxy differs in mass, size, brightness, stellar populations and morphology. This is exactly why we have created systems to classify them.
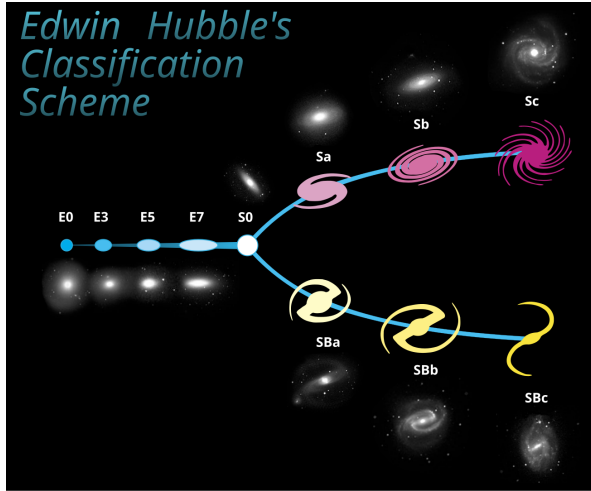
Galaxy Classification

One of the most common methods of classification is the *Hubble classification (Hubble 1925)* , which categorizes galaxies based on their morphology.

- **Elliptical Galaxies (E):** Ellipsoidal shapes with smooth brightness profiles, containing older stars and minimal interstellar matter. Their eccentricity takes values from 0 to 0.7, so we can categorize them even further, form E0 to E7

- **Lenticular Galaxies (S0):** Intermediate between elliptical and spiral galaxies, featuring a central bulge and disk but lacking significant spiral structure.

- **Spiral Galaxies:** Characterized by a central bulge and spiral arms. Depending on the arm tightness we can categorize them as *a,b,c,d* from tight to looser, and depending if they have a bar or not they are subdivided into:

---

[1]Hoskin (1976)

– **Unbarred Spirals (S):** No central bar; classified as Sa, Sb, Sc, etc., based on arm tightness and bulge size.

– **Barred Spirals (SB):** Feature a central bar; denoted as SBa, SBb, SBc, etc.

- **Irregular Galaxies (Irr):** Lack regular structure, often rich in gas and dust with high star formation rates.

(a) Tuning-fork-style diagram of the Hubble sequence By Cosmogoblin - Own work, CC0. https://commons.wikimedia.org/w/index.php?curid=121743256
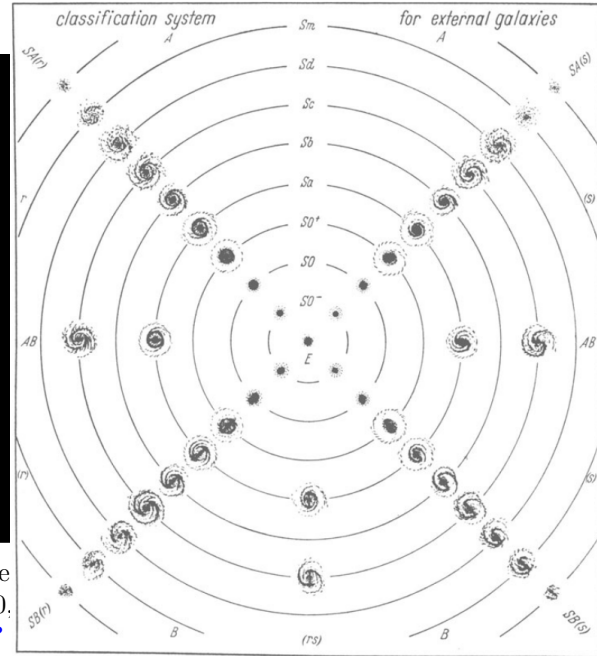
(b) Hubble-de Vaucouleurs classification system By de Vaucouleurs (1959)

Figure 1: Diagrams visualizing the Hubble and Hubble-de Vaucouleurs morphological classification systems

Although Hubble's original scheme was revolutionary, **de Vaucouleurs** recognized that not all galaxies fit neatly into its categories. In response, he introduced a more nuanced classification system (de Vaucouleurs 1959) that:

- **Accounts for Rings**: Some galaxies feature ring-like structures around their bulge or bar. To denote this, de Vaucouleurs added **(R)** to the classification (for example, (R)SBa).

- **Differentiates Bar Strength**: Since bars can vary from subtle to dominant, he proposed **SA** (unbarred), **SAB** (weakly barred), and **SB** (strongly barred).

- **Incorporates Numerical Types (T-Types)**: To capture subtle transitions along the morphological sequence, de Vaucouleurs assigned a numerical index (T) ranging from

-6 (pure compact ellipticals) to +10 (extreme irregulars). Intermediate values (e.g., -1 for S0, 2 for Sab, 5 for Sc, etc.) let astronomers pinpoint galaxies that don't fit cleanly into the original categories.

This expanded framework also embraces **early-type** and **late-type** galaxies as part of a continuous evolutionary sequence:

- **Early-type galaxies** (E and S0):

    - Smooth appearance.

    - Predominantly older stellar populations.

    - Minimal amounts of gas and dust.

    - Assigned negative T-values ($-6 \leq T < 0$).

- **Late-type galaxies** (Spirals and Irregulars):

    - Rich in gas and dust.

    - Significant ongoing star formation.

    - Smaller bulges and more open arms from Sa/SBa to Sc/SBc.

    - Assigned positive T-values , extending to +11 for extreme irregulars.

By offering extra designations for bar strength, ring features, and transitional morphologies, de Vaucouleurs' system paints a more complete picture of galaxies and how they evolve. It allows researchers to quantify where a galaxy lies along the continuum, rather than forcing it into a single rigid label.

Table 1: This table was based on the LaTeX files of ("RC3 - Third Reference Catalog of Bright Galaxies" n.d.)

Hubble	E	E-S0	S0	S0/a	Sa	Sa-b	Sb	Sb-c	Sc	Sc-Irr	Irr
T	-5	[-4,-3]	[-2,-1]	0	1	2	3	4	[5,6,7]	8	[9,10,11]

Dwarf Galaxies

Despite the usefulness of de Vaucouleurs' numerical T-type system , we run into practical issues when classifying dwarf galaxies. These galaxies need a more detailed classification system, since the T-Type system can denote galaxies, whose physical properties drastically differ, with by the same number. For instance, dwarf spheroidals and normal ellipticals both end up with a T-value below zero (T < 0), even though their properties are vastly different. Then there are "transient" dwarf galaxies (Tr), whose features bridge spheroidal (Sph)(Sph) and irregular (Ir)(Ir) types. Inaccuracies in classification can cause these hybrids to "jump" from one extreme of the T-scale to the other with only a small error in morphology.

To address this, van den Bergh suggested dividing dwarf galaxies by luminosity class, which prevents them from leaping between extreme categories. This refined approach better reflects the intrinsic diversity of dwarf systems, ensuring that subtle morphological differences are more accurately captured and reducing the risk of placing galaxies at the wrong end of the classification scale (Karachentsev, Makarov, and Kaisina 2013)

Star-Forming Regions

One of the main ingredients of the galaxies are large scale molecular clouds, rich in hydrogen, with masses of order 10^5 $M_\odot$, typical dimensions of ~ 10 parsec, temperatures of 10-100 K and densities of 10-300 molecules/cm^3 (Pols 2009). Stars are created inside these clouds when a perturbation disturbs them, and thus their pressure equilibrium, and they start to collapse into smaller clouds under their self-gravity.

The collapse leads to the formation of protostars, which eventually become main-sequence stars. The presence of dust within these clouds is crucial, as it shields the interior regions from ultraviolet radiation, allowing the gas to cool to temperatures below 100 K, facilitating star formation .

The location of the star forming regions within a galaxy depend on the morphology. In spiral galaxies, star formation mainly occurs along the disk, where the molecular clouds are dense due to the compression caused by spiral density waves. The compression not only initiates the collapse of the clouds and thus the star formation, but also feeds the arms with gas, which sustains the star formation.

In elliptical galaxies, on the other hand, star formation is minimal because they lack the cold gas reservoirs needed for new stars to form. Irregular galaxies, with their chaotic structures, often have patchy but vigorous star-forming regions, as they retain significant amounts of gas.

A special case are the starburst galaxies, who have a extremely active star forming regions, and seem to convert the gas into stars extremely fast (even 100 times faster than the Milky Way). These starbursts often concentrate their intense star-formation activity in compact

regions about 1 kpc in size (typically in galaxy nuclei). Due to their high star-formation rates, starbursts host large numbers of young stars.

Star Formation History (SFH)

The SFH of a galaxy describes the evolution of its star formation rate over time. By selecting an appropriate model for SFH, we can analyze stellar production, predict periods of active or quiescent star formation, and determine when SFR stabilizes.

Understanding SFH models is crucial for interpreting internal and external processes affecting galaxies and identifying conditions for intense star formation in their early stages.

Star Formation Rate

The star formation rate (SFR) is defined as the total gas mass of a galaxy converted into stars over a specific time interval. It is typically expressed in solar masses per year ($M_\odot \cdot \mathrm{yr}^{-1}$).

The SFR varies significantly over time, and its integration over time provides the total stellar mass formed during the galaxy's history of star formation. Specifically:

$$\int_0^{t_{sf}} \mathrm{SFR}(t)dt = \zeta M_*(t_{sf}), \ t_{sf} = \text{Time of Star Formation}, \tag{1}$$

where ζ accounts for mass loss during the Star Formation and is approximately $\zeta \approx 1.3$ (Kroupa et al. (2020)).

It is also important to define the Star Formation Density (SFRD):

$$\mathrm{SFRD} = \frac{1}{V} \sum_{i=1}^{N} \mathrm{SFR}_{o,i},$$

where V is the comoving volume [2] of a region of the universe, N is the number of galaxies of the regions and $\mathrm{SFR}_{0,i}$ is the current SFR of each galaxy i.

For the Local Cosmological Volume, which we will focus on, the volume is the sphere with its center at the Milky Way and a radius of 11 Mpc $V = \frac{4}{3}\pi(11\,\mathrm{Mpc})^3 \approx 5575.3\,\mathrm{Mpc}^3$.

---

[2]Comoving volume factors out the expansion of the universe, it remains a constant measure of "space" over time, making it possible to compare star formation at different epochs

Estimating SFR from Spectra

SFR can be estimated using various photometric or spectroscopic methods based on the luminosity of at least one spectral band or the intensity of a spectral line. Different luminosities and intensities trace distinct emission mechanisms, offering insights into a galaxy's radiation sources. Below are common methods:[3]

- **H α Emission**: Young, hot, massive stars (O-type stars, ~10 Myr, ~20 $M_\odot$) produce a number of ionizing photons, which they ionize the surrounding hydrogen rich gas. The hydorgen undergoes recombination cascades which produce Balmer emission lines of $H\alpha$ (0.6563 μm) and $H\beta$ (0.4861 μm). Dust can significantly affect observations.

- **Far-Ultraviolet (FUV) Flux**: Mainly emitted by young, hot stars (B-type stars, ~100 Myr). Dust presence can also significantly affect observations.

- **Infrared (IR) Flux**: The stars in a galaxy can heat up the dust in different ways, which then emits radiation in different parts of the IR spectrum. For example, young and massive, short-lived stars, emit UV radiation which then the heated dust emits in a wavelength of $\approx 60 \mu m$, whereas dust heated by UV-faint old or low-mass stars will emit at $\approx 100 - 150 \mu m$. As a result, the total IR emission is age-agnostic and provides a more accurate approximation of the SFR because it accounts for contributions from both young and old stellar populations.

- **Radio Continuum Emission**: Strongly correlated with IR. Its origin is complex, involving synchrotron radiation from relativistic electrons and thermal Bremsstrahlung from hot gas.

- **X-Ray Emission**: In star-forming galaxies, X-rays arise from high-mass binary systems (neutron star or black hole with massive stellar companion) and hot gas from supernovae, correlating with SFR up to redshift $z \sim 4$. X-rays are dust-insensitive, enabling accurate high-redshift observations.

SFR for different luminosities L_i can be calculated as:

$$\mathrm{SFR}_i = \mathcal{K}_i \times L_i \tag{2}$$

where $\mathcal{K}_i$ is a constant specific to each L_i ($i = $ Hα, IR, radio, FUV, X). In our analysis, we lack radio and X-ray data.

Since the luminosities L_{FUV} and $L_{\mathrm{H}\alpha}$ originate from young stars and are highly sensitive to dust, we either directly observe stars unaffected by dust or use correction models to account for dust absorption. It is crucial to ensure that these models neither underestimate nor overestimate the luminosities by overlooking or double-counting the same sources.

---

[3]Calzetti (2012), Mushotzky (2017)

Additionally, because these luminosities are emitted by similar stellar populations, we can reasonably expect the SFR_{FUV} and $SFR_{\mathrm{H}\alpha}$ to be approximately equal. As shown in the data from (Karachentsev and Kaisina 2013) and supported by (Kroupa et al. 2020), a suitable approach for estimating the total SFR from FUV and Hα observations is to calculate their average:

$$SFR_{\mathrm{FUV},H\alpha} = \mathrm{mean}(SFR_{\mathrm{FUV}}, SFR_{\mathrm{H}\alpha}) \tag{3}$$

where L_{FUV} and $L_{\mathrm{H}\alpha}$ are corrected for dust attenuation.
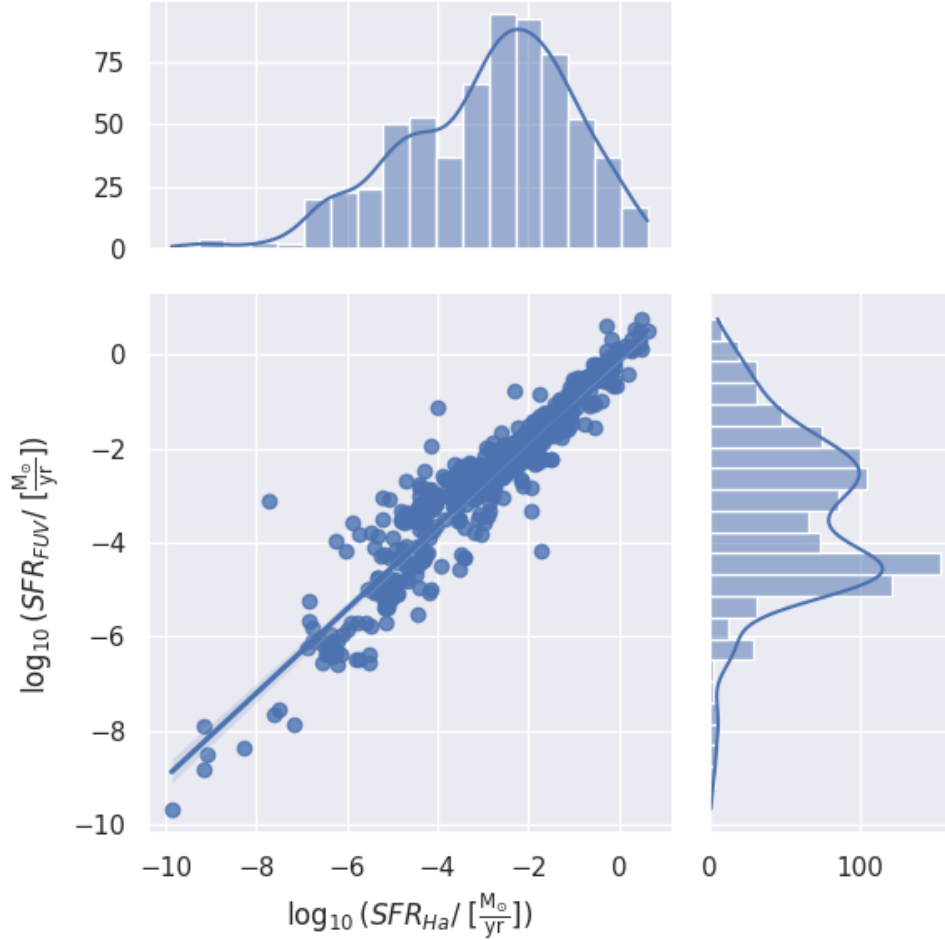

Figure 2: Plot showing the linear relation $\log_{10} \mathrm{SFR}_{FUV} = \log_{10} \mathrm{SFR}_{H\alpha}$, as well as their distrubutions

10

According to (Madau and Dickinson 2014), this method often underestimates the SFR, since different galaxy populations may systematically follow distinct absorption mechanisms depending on their characteristics.

Since SFR_{FUV}, based on the uncorrected L_{FUV}, represents the emission from unobstructed stellar populations, and SFR_{TIR} isaccounts for dust-reprocessed light, a more accurate way to calculate the total SFR of a galaxy is:

$$SFR_{\mathrm{total}} = \mathcal{K}_{\mathrm{FUV}} \cdot L_{\mathrm{FUV}} + \mathcal{K}_{\mathrm{IR}} \cdot L_{\mathrm{IR}} \tag{4}$$

Following the same reasoning as the previous formula, the total SFR can be expressed as:

$$SFR_{\mathrm{total}} = \mathrm{mean}\left(\mathcal{K}_{\mathrm{FUV}} \cdot L_{\mathrm{FUV}}, \mathcal{K}_{\mathrm{H\alpha}} \cdot L_{\mathrm{H\alpha}}\right) + \mathcal{K}_{\mathrm{IR}} \cdot L_{\mathrm{IR}} = SFR_{\mathrm{FUV}, H\alpha} + SFR_{\mathrm{IR}}$$

where L_{FUV} and $L_{\mathrm{H\alpha}}$ are not corrected for dust absorption. However, since we do not have enough galaxies with both traces, we will use a different method of calculating the total SFR, which we will discuss later.

Main Sequence Galaxies

The SFR and stellar mass of a galaxy are tightly correlated by the relationship:

$$\log(\mathrm{SFR}) = \alpha \log(M_*) + \beta$$

where $\alpha(t)$ and $\beta(t)$ depend on time and redshift z (Speagle et al. (2014)):
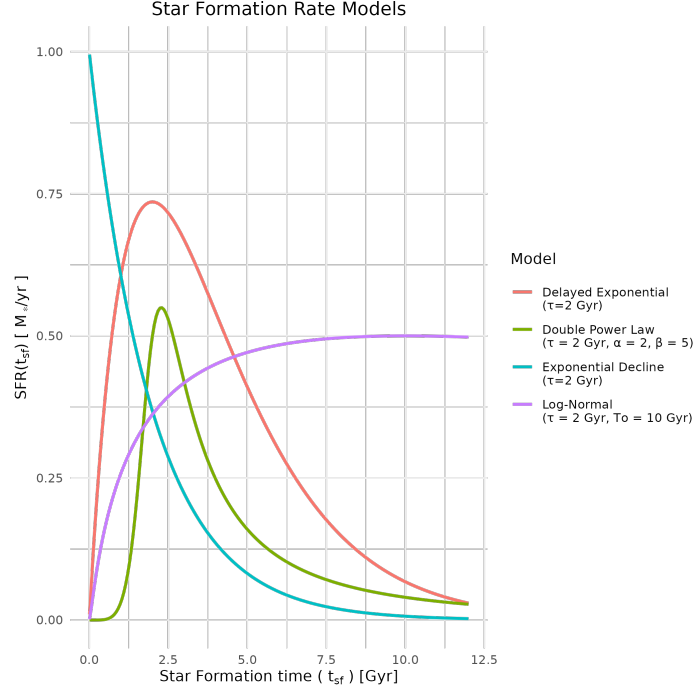
Star Formation History Models

Figure 3: Star Formation Rate over the time of star formation, for different parametric models

Parameterized SFH models are commonly used, offering simplicity through a few parameters (Carnall et al. 2019):

- **Exponential Decline (Tau Model):** The star formation rate (SFR) decreases exponentially over time, following the equation:

$$\mathrm{SFR}(t) \propto e^{-t_{\mathrm{sf}}/\tau}$$

where τ is the timescale, $t_{\mathrm{sf}} = t - T_0$ is the star formation time, t is the age of the Universe, and T_0 is the time when star formation began.

- **Delayed Exponential (Delayed Tau Model):** This model provides a more complex representation where the SFR initially increases, reaches a peak, and then declines exponentially over time. The equation for this model is:

$$\mathrm{SFR}(t) \propto t_{\mathrm{sf}} e^{-t_{\mathrm{sf}}/\tau}$$

12

This accounts for an initial growth phase followed by a decline. In this case, τ represents the time it takes for the galaxy to reach $\mathrm{SFR_{max}}$.

- **Log-Normal Distribution Model:** The SFR follows a normalized log-normal distribution, which can accurately model the star formation rate density ($\mathrm{SFRD = SFR}/M_*$) in individual galaxies. The general form of the equation is:

$$\mathrm{SFR}(t) \propto \frac{1}{\tau} \exp \left(-\frac{(\ln(t) - T_0)^2}{2\tau^2} \right)$$

where τ and T_0 are free parameters of the distribution that lack physical significance, as the SFR does not necessarily peak at $t = e^{T_0}$.

- **Double Power Law:** This model describes a scenario where the SFR rises and then falls sharply, useful for modeling galaxies experiencing rapid changes in star formation. The equation is:

$$\mathrm{SFR}(t) \propto \left[\left(\frac{t}{\tau} \right)^{\alpha} + \left(\frac{t}{\tau} \right)^{\beta} \right]^{-1}$$

where τ is the timescale and α, β are exponents that govern the rise and fall of the SFR.

Additionally, there are non-parametric models, which do not follow a specific functional form to describe the star formation of a galaxy. These models are more flexible in adapting to galaxies with more complex star formation patterns.

Lilly-Madau Plot and Delayed-τ model conflicts

The Lilly-Madau plot is one of the most important plots in the field of galaxy evolution. It describes how the SFRD of the universe evolved over time, with observational data. But to understand it, we first need to understand how the observed age of the Universe and the redshifts of galaxies are related.

Redshift and lookback time

According to Hubble–Lemaître law, all the galaxies are moving away from each other, at a speed proportional to their distance, due to the expansion of the universe.

$V = H_0 \times d$, where $H_0 \approx 69.8$ km/s/Mpc is the Hubble constant and d is the distance between the two galaxies.[4]

Since we have galaxies with relative motions emitting light waves, we can observe the Doppler effect. Specifically, since the galaxies are moving away from each other, and thus from us also, we observe radiation with longer wavelenghts.

Redshift (z) is the doppler shift resulting from radial motion:

$$z = \frac{\lambda_{observed}}{\lambda_{emitted}} - 1$$

In special relativity, z is related to radial velocity v by (Hogg 2000)

$$1 + z = \sqrt{\frac{1 + v/c}{1 - v/c}} \tag{5}$$

For small v/c we can rewrite Equation 5, as:

$$z \approx \frac{V}{c} = \frac{H_0 \times d}{c}$$

But, because light takes time to cover the distance d between two galaxies, when the light finally reaches as, we will see the observed galaxy, as it was when the light was emitted, and not how it is at this moment. If we substitute time that it took the light to reach us over the distance, then we arrive at the relation (Longair 1998):

$$t_{\text{emitted}} \propto z^{-3/2}$$

The lookback time is the difference between the current age of the Universe and the age of the Universe when the light was emitted

$$t_L = T_0 - t_{\text{emitted}}$$

---

[4]We also have non-Hubble motions $V = H_0 \times d + V_0$, where V_0 is the peculiar velocity and it could, for example, be due to galaxy cluster dynamics. For the current explanation we are going to ignore it. This way the radial velocity v is equal to V
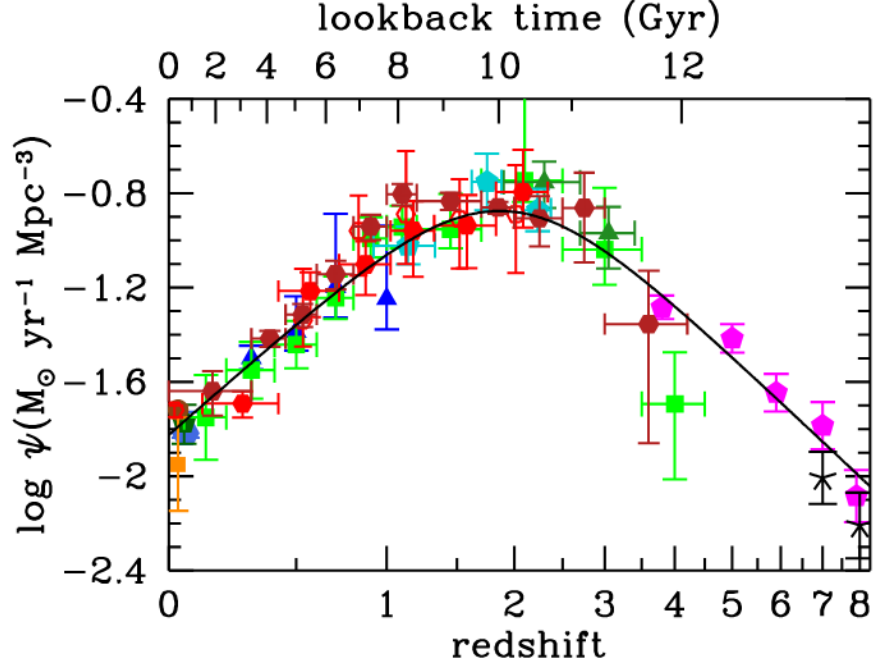
Lilly-Madau Plot

Figure 4: The history of cosmic star formation as shown in Madau and Dickinson (2014)

Using observational data from UV and IR traces for the SFR for galaxies of different redshifts (z) Madau and Dickinson (2014) where able to calculate the cosmic SFRD, at different ages of the universe, and reveals three periods of the universe.

- **Rising Era** (SFRD$\propto (1+z)^{-2.9}$, $3 \lesssim z \lesssim 8$): The SFRD is relatively low at very high redshifts (e.g., $z > 6$) and then rises as we move closer to $z \sim 2$. This indicates that early galaxies were ramping up their star-forming activity.

- **Peak Star Formation** ($z \sim 2$): Often dubbed "cosmic noon," this epoch exhibits the highest SFRD in cosmic history when the Universe was ~ 3.5 Gyr old. Galaxies are vigorously converting gas into stars, and many of the most massive galaxy systems today formed much of their stellar content during this phase.

- **Decline to Present Day** (SFRD$\propto (1+z)^{2.7}, z \lesssim 2$): After $z \sim 2$, the global SFRD drops by about an order of magnitude towards the present day ($z = 0$).

The best-fit function of the comoving SFRD(z):

$$SFRD(z) = 0.015 \frac{(1+z)^{2.7}}{1+\left(\frac{1+z}{2.9}\right)^{5.6}} \quad \left[M_\odot \,\mathrm{yr}^{-1}\,\mathrm{Mpc}^{-3}\right],$$

Delayed-τ model

The delayed τ model is widely used for describing an initial starburst followed by a gradual decline in SFR. This places galaxies on the main sequence. It is particularly effective for massive galaxies (Haslbauer, Kroupa, and Jerabkova (2023)). However, it assumes smooth SFR evolution and may overestimate peak SFR in high-redshift galaxies.

Using the delayed model, we compute τ, t_{sf}, and normalization constant A_{del} with:

$$\mathrm{SFR}_0 = \mathrm{SFR}(t_{sf}) = A_{del} \frac{t_{sf}}{\tau^2} e^{-t_{sf}/\tau} \tag{6}$$

where SFR_0 is given in the catalogs.

Computational Methods

Newton-Raphson

Markov Chain Monte Carlo

Prepering the Catalogs

UNGC HECATE join etc...

Catalog Completeness

Comparing the Catalogs

The "special" case of the Star Formation Rates

Calculating the parameters

According to pre-existing bibliography

Problems with the method

MCMC

Calzetti, Daniela. 2012. "Star Formation Rate Indicators." arXiv. https://arxiv.org/abs/1208.2997.

Carnall, Adam C., Joel Leja, Benjamin D. Johnson, Ross J. McLure, James S. Dunlop, and Charlie Conroy. 2019. "How to Measure Galaxy Star Formation Histories. I. Parametric Models." *The Astrophysical Journal* 873 (1): 44. https://doi.org/10.3847/1538-4357/ab04a2.

de Vaucouleurs, Gerard. 1959. "Classification and Morphology of External Galaxies." *Handbuch Der Physik* 53 (January): 275. https://doi.org/10.1007/978-3-642-45932-0_7.

Haslbauer, Moritz, Pavel Kroupa, and Tereza Jerabkova. 2023. "The Cosmological Star Formation History from the Local Cosmological Volume of Galaxies and Constraints on the Matter Homogeneity." *Monthly Notices of the Royal Astronomical Society* 524 (3): 3252–62. https://doi.org/10.1093/mnras/stad1986.

Hogg, David W. 2000. "Distance Measures in Cosmology." arXiv. https://doi.org/10.48550/arXiv.astro-ph/9905116.

Hoskin, Michael A. 1976. "The 'Great Debate': What Really Happened Page."

Hubble, E. P. 1925. "Cepheids in Spiral Nebulae." *The Observatory* 48 (May): 139–42.

Karachentsev, Igor D., and Elena I. Kaisina. 2013. "STAR FORMATION PROPERTIES IN THE LOCAL VOLUME GALAXIES VIA Hα AND FAR-ULTRAVIOLET FLUXES." *The Astronomical Journal* 146 (3): 46. https://doi.org/10.1088/0004-6256/146/3/46.

Karachentsev, Igor D., Dmitry I. Makarov, and Elena I. Kaisina. 2013. "UPDATED NEARBY GALAXY CATALOG." *The Astronomical Journal* 145 (4): 101. https://doi.org/10.1088/0004-6256/145/4/101.

Kroupa, P, M Haslbauer, I Banik, S T Nagesh, and J Pflamm-Altenburg. 2020. "Constraints on the Star Formation Histories of Galaxies in the Local Cosmological Volume." *Monthly Notices of the Royal Astronomical Society* 497 (1): 37–43. https://doi.org/10.1093/mnras/staa1851.

Leavitt, Henrietta S. 1907. "1777 Variables in the Magellanic Clouds." *Annals of Harvard College Observatory* 60: 87–108.3.

Longair, Malcolm S. 1998. *Galaxy Formation.* Springer Science & Business Media.

Madau, Piero, and Mark Dickinson. 2014. "Cosmic Star Formation History." *Annual Review of Astronomy and Astrophysics* 52 (1): 415–86. https://doi.org/10.1146/annurev-astro-081811-125615.

Mushotzky, Richard. 2017. "ASTR620 Galaxies - Fall 2017." Lectures. University of Maryland.

Pols, Onno. 2009. *Stellar Structure and Evolution.* Utrecht University.

"RC3 - Third Reference Catalog of Bright Galaxies." n.d. https://heasarc.gsfc.nasa.gov/w3browse/all/rc3.html. Accessed December 28, 2024.

Shapley, Harlow, and Heber D. Curtis. 1921. "The Scale of the Universe." *Bulletin of the National Research Council* 2 (11): 171–217.

Speagle, Joshua S., Charles L. Steinhardt, Peter L. Capak, and John D. Silverman. 2014. "A Highly Consistent Framework for the Evolution of the Star-Forming "Main Sequence" from z~0-6." *The Astrophysical Journal Supplement Series* 214 (2): 15. https://doi.org/10.1088/0067-0049/214/2/15.